

Full length article

Label-free non-invasive classification of rice seeds using optical coherence tomography assisted with deep neural network



Deepa Joshi ^{a,1,*}, Ankit Butola ^{a,1}, Sheetal Raosaheb Kanade ^a, Dilip K. Prasad ^c, S. V. Amitha Mithra ^b, N.K. Singh ^b, Deepak Singh Bisht ^b, Dalip Singh Mehta ^{a,*}

^a Bio-photonics Laboratory, Department of Physics, Indian Institute of Technology Delhi, Hauz-Khas, New Delhi 110016, India

^b National Institute for Plant Biotechnology, NIPB, PUSA, New Delhi 110012, India

^c Department of Computer Science, UiT The Arctic Univ. of Norway, Tromsø, Norway

ARTICLE INFO

Keywords:

Rice

Optical coherence tomography

Deep learning

Seed

Non-contact

Structure of Abstract

1. Background
2. Existing method
3. Problem
4. Given solution
5. Findings
6. Implication

ABSTRACT

Identification of the seed varieties is essential in the quality control and high yield crop growth. The existing methods of varietal identification rely primarily on visual examination and DNA fingerprinting. Although the pattern of DNA fingerprinting allows precise classification of seed varieties but fraught with challenges such as low rate of polymorphism amongst closely related species, destructive method of analysis and a huge cost involved in identification of robust markers such as simple sequence repeat (SSR) and single nucleotide polymorphisms. Here, we propose a fast, non-contact and non-invasive technique, deep learning assisted optical coherence tomography (OCT) for subsurface imaging in order to distinguish different seed varieties. The volumetric dataset of, (a) four rice varieties (PUSA Basmati 1, PUSA 1509, PUSA 44 and IR 64) and, (b) seven morphologically similar seeds of rice landrace Pokkali was acquired using OCT technique. A feedforward deep neural network is implemented for deep feature extraction and to classify the OCT images into their relevant classes. The proposed method provides the classification accuracy of 89.6% for the dataset of total 158,421 OCT images and 82.5% in classifying the dataset of total 56,301 OCT images collected from Pokkali seeds. The current technique can accurately classify seed varieties irrespective of the morphological similarities and can be adopted for the removal of varietal duplication and assessment of the purity of the seeds.

1. Introduction

Rice (*Oryza sativa* L.) is a staple food for more than half of the world's population providing 55–80% of total calories for people in Asia, Africa and Latin America [1]. Abundant crop harvest is required to cater the global food demand in the growing world population [2]. For the development of new high-yielding crop varieties, quality of seed is accorded as a topmost priority in plant breeding programs because it is the primary determinant of seedling vigour, subsequent plant growth and performance. The expectation of abundant harvest from a piece of agricultural land can be achieved if the seed is true to the selected variety. In addition, before the entry of seeds into the market chain, several other seed certification measures are also undertaken to minimize the co-mingling of undesirable seeds, other crop or weed seeds. However, because of the abundant intra-varietal genetic diversity in rice [3], the challenge of duplication in the submitted accessions of released

varieties, germplasms and landraces is faced by gene banks, which act as a source of seeds for plant breeding programs [4]. Knowing accurately the type of seed beforehand can help ensure its efficient utilization in the plant breeding research programs.

The varietal identification relies on visual inspection and the results of distinctness, uniformity and stability (DUS) testing. On the basis of DUS testing, a variety before its commercial release has to be categorized distinct for any other previously released varieties and should be uniform and stable for other morphologically evaluated traits. However, in the present context, where large number of crop varieties are already available, establishing distinctiveness of any new variety solely on the basis of DUS testing often becomes challenging. In such cases, DNA profiling of varieties via molecular markers may complement the DUS testing results. There are several classes of robust DNA based markers including simple sequence repeat (SSR) and single nucleotide polymorphisms (SNP) markers that can be used for DNA profiling [5].

* Corresponding authors.

E-mail addresses: ird12512@iitd.ac.in (D. Joshi), mehtads@physics.iitd.ac.in (D.S. Mehta).

¹ These authors contributed equally to this work.

However, despite the robustness and precision of DNA fingerprinting, its utility is largely confined to identify varieties where enough sequence information is already available across the databases. Primarily because designing of the SSR and SNP markers in the crops with scarce genome resources is cost intensive [6]. In addition, destructive method adopted while processing samples for DNA isolation and time involved also limits its application in several cases.

Non-destructive methods are widely used to account for the duplication amongst the submitted accessions of released varieties, germplasms and landraces in the seeds obtained from the gene banks [4]. Several rapid and non-destructive image processing-based approaches have been proposed to address this in the recent years such as digital images analysis [7], magnetic resonance imaging (MRI) [8], positron emission tomography (PET) [9], X-rays, confocal microscopy [10,11], NIR spectroscopy [12] and hyperspectral imaging [13,14]. In digital image analysis technique red, green and blue (RGB) histogram of a captured 2D image is plotted for the rice seed identification. Since the technique can offer only 2D digital images and the colour histogram of the seed, it cannot provide subcellular morphological changes inside the seed and thus not yet applicable to classify between alike seeds. Secondly, NIR spectroscopy and hyperspectral imaging offers the chemical specificity of the sample but still limited to the 2D surface only. In summary, trade-off between low resolution, long acquisition time and limited penetration depth of these alternative approaches motivated us, for a deep learning assisted OCT based method with increased sensitivity and resolution for rice seeds identification. Rice is a crop with immense genetic diversity. So far varietal identification is generally done by visual screening or with the genetic testing using DNA markers. Theoretically we have to develop a database for each of the variety, if our goal is mainly for varietal breeding or any other related research activities. However, for seed companies a database harbouring information on some of the leading mega-varieties will suffice. Since the variations among the seeds of the same variety is a primary concern of farmers and plant breeders, addition of another dimension of proposed sub-surface imaging might assist in developing the reference calibration machine models for seed identification.

Optical coherence tomography OCT is a non-contact and non-invasive 3D imaging technique and is growing tremendously for medical and agricultural imaging. OCT can image with axial and transverse resolution of 12 μm and 16 μm respectively. Technological advancements in OCT make it feasible and widely popular for its adoption in various biological and biomedical applications such as early detection of cancer [15], ophthalmology [16] and dentistry [17,18]. In addition, OCT has also been employed in past for several agricultural applications such as of quality assessment of leaf and fruit samples [19,20], disease progression [21,22] and varietal classification [23]. Moreover recent OCT studies in Apple [24], plant tissues [25] and rice leaf [26], tomato [27] has confirmed OCT as a promising imaging modality for Agri-photonics. Successful incorporation in agriculture has carved out a ubiquitous place for OCT among its comparable counter imaging techniques.

In this study, we propose swept source optical coherence tomography (SS-OCT) [28] for volumetric imaging of different varieties of seed. In order to classify the rice seeds using proposed method, we acquired a total of 158,421 OCT images from 200 seeds (50 of each class) of Group I dataset i.e. PUSA Basmati 1, PUSA 1509, PUSA 44 and IR 64. Also, total 56,301 OCT imaged from 280 seeds (40 from each class) of rice landrace Pokalli (Group II dataset). Further, the cutting-edge artificial intelligence image processing techniques i.e. transfer learning is utilized to accurately extract relevant information from the complex datasets. The performance of the trained network is evaluated against the test datasets of both Group I and II. Our current framework achieves 89.6% testing accuracy for classifying the Group I and 82.5% classification accuracy for Group II dataset. The Group I varieties also cross validated by DNA profiling based on randomly chosen seven Hyper variable simple sequence repeat markers (HvSSRs). The current approach combining

OCT with deep learning [29] will be a functional step for the more accurate identification of seed varieties with broader application in the seed industry.

2. Materials and methods

2.1. Experimental setup

Micro-electro-mechanical system vertical-cavity surface-emitting laser (MEMS-VCSEL) based swept-source central optical coherence tomography (SS-OCT) system (OCS1310V1-1300 nm) [28] is used for imaging the rice varieties. OCT is a non-invasive real-time 3D imaging technique that works on the principle of low-coherence interferometry [18]. The schematic of the experiment setup of the SS-OCT system is shown in Fig. 1. The sweeping range from 1285 to 1315 nm with central wavelength of 1300 nm is used in the present study. The source contained a MEMS tunable VCSEL and a 10-dB spectral bandwidth of 100 nm included a Mach-Zehnder interferometer “k-clock” for optical clocking data acquisition. The light beam is coupled into 50:50 fiber coupler to split it into two parts i.e. reference and sample beam. The sample beam illuminates the specimens with average output power of 25mW by passing through a microscope objective (MO, LSM03, Thorlabs, focal length ~25.1 mm in air) lens. The back-reflected light of the sample beam interferes with the reference beam and contains the depth information of the sample at particular point called A-scan (1D scan). Further XY galvo scanner scans the sample along any particular direction (say X direction) to acquire multiple A-scans. These adjacent A-scans are combined to get 2D (XZ) information of the sample called B-scan. The system offers axial and transverse resolutions of 12 μm and 16 μm in air, respectively. The 3D or volumetric image can be obtained by combining multiple B-scan images obtained by scanning XY scanner in the Y direction. Field of view in XY dimension is limited by the objective lens of the system while the Z dimension limits by the depth of penetration of the light.

2.2. Seed sample details

The rice seed samples used in the present investigation were obtained from National Institute of Plant Biotechnology, New Delhi, India. For OCT analysis the seeds were grouped into two categories; (a) Group I comprised of four rice varieties (PUSA Basmati 1, PUSA 1509, PUSA 44 and IR64) having significant morphological difference, and (b) Group II consists of seven accessions (BJJ-10-1, BJJ-10-2, BJJ-10-4, BJJ-10-6, BJJ-10-8, BJJ-10-9 and Vyttila 6) of rice landrace Pokalli indistinguishable by visual inspection (see Fig. 2). All the seeds used in the present study were one year old. For OCT analysis no preconditioning is required so the seeds were imaged directly. The seeds of different varieties had an approximate size of 7 mm \times 3 mm \times 2 mm (length \times width \times height). Total 50 seed samples for each class of Group I were volumetrically imaged using OCT at two distinct random locations. Similarly, 40 seed samples for each class of Group II were imaged using OCT at two distinct random locations. Each volumetric (3D) OCT image corresponds to 1.5 mm \times 1.5 mm \times 2 mm in x-y-z direction and contains 400 B-scans (2D x-z sections) for Group I and approximately 100 B-scans for Group II. In this manner, a large dataset of 160,000 OCT images of Group I were obtained. However, few images of Group I samples are discarded to avoid unwanted mechanical error due to galvo scanner and total 158,421 B-scan images are used. Similarly, total 56,301 OCT images for Group II were obtained. The OCT images were acquired one at a time, each 3D image acquisition takes approximately 80–100 s, using Thorlabs OCT software which can be rendered in the form of 2D images when exported. Every 2D image is saved in BMP format and has an approximate size of 833 KB (see Fig. 4).

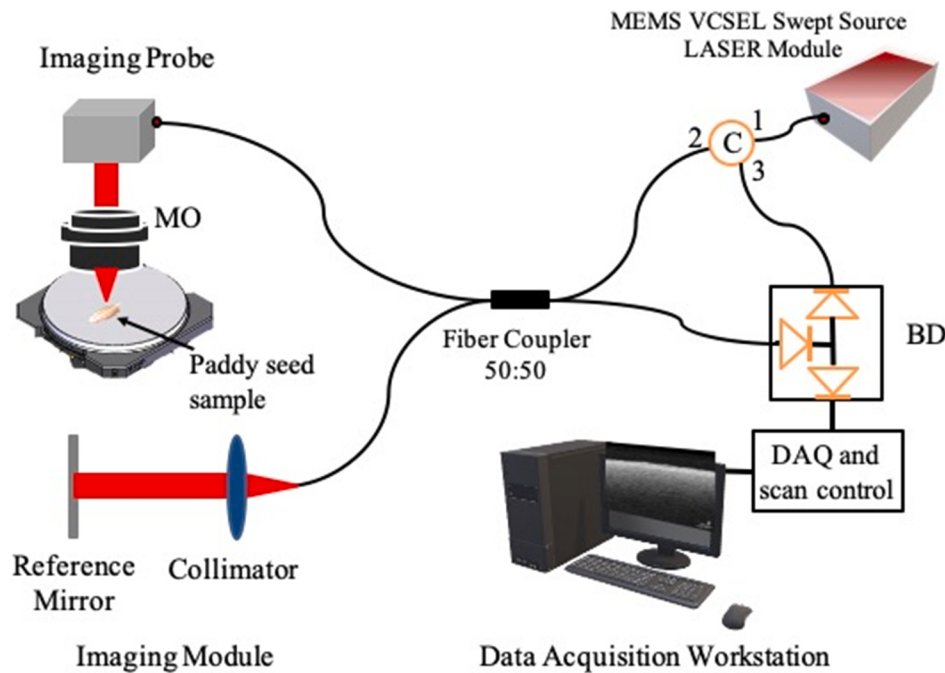


Fig. 1. Schematic diagram of Micro electro-mechanical system-vertical cavity surface emitting laser (MEMS-VCSEL) based swept-source optical coherence tomography (SS-OCT) system [28] for the classification of paddy seeds. Imaging probe contains the X-Y galvanometers and optics required to manipulate the swept laser onto the paddy seeds (imaging sample).

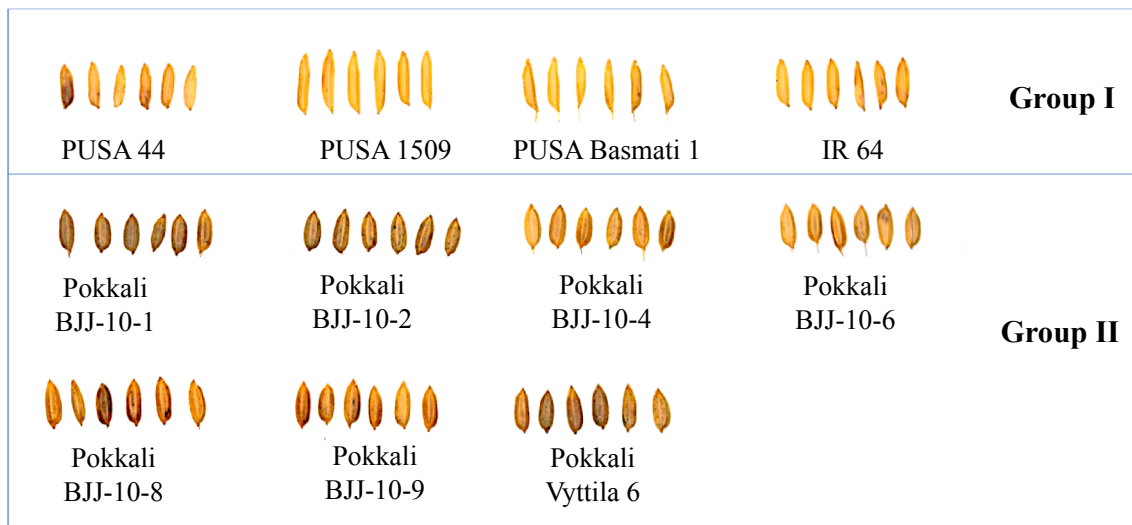


Fig. 2. Images of different rice varieties used in the present investigation captured by mobile phone camera.

2.3. Workflow of the proposed method

The workflow of the framework using conventional SS-OCT and transfer learning approach is elaborated in Fig. 3. The bright-field images of all the samples shown in Fig. 3 (a), were imaged using SS-OCT system (see Fig. 3(b)). Each B-scan OCT image corresponds to 1.5×2 mm physical dimension in XZ direction. The detail to the datasets and experimental system are given in Sections 2.1 and 2.2. The obtained B-scan images were fed into the Inception-ResNet-V2 architecture for training (see Fig. 3 (c)). The details of the network are mentioned in Section 2.4. Last three layers of the architecture were further modified to retrain it on the rice datasets. After the training, the test dataset captured from completely different rice seed is used to check the performance of the network. The testing performance is summarized in the form of

confusion matrix [30], symbolized in Fig. 3(d). Confusion matrix is a common way to represent the correct and incorrect testing prediction of the network. In the confusion matrix, the diagonal elements represent the correct predictions while the off-diagonal elements correspond to incorrect predictions of the network.

2.4. Data analysis using Inception-ResNet-V2 architecture

In a recent years, conventional feature extraction algorithms are proposed to classify the datasets [31,32]. However, extracting the features from the data often relies on the human interpretation of structural and visual features of the sample such as length, width, area, colour, texture in context of seed classification [33]. In contrast, in deep learning the features are extracted by feeding sufficient training data

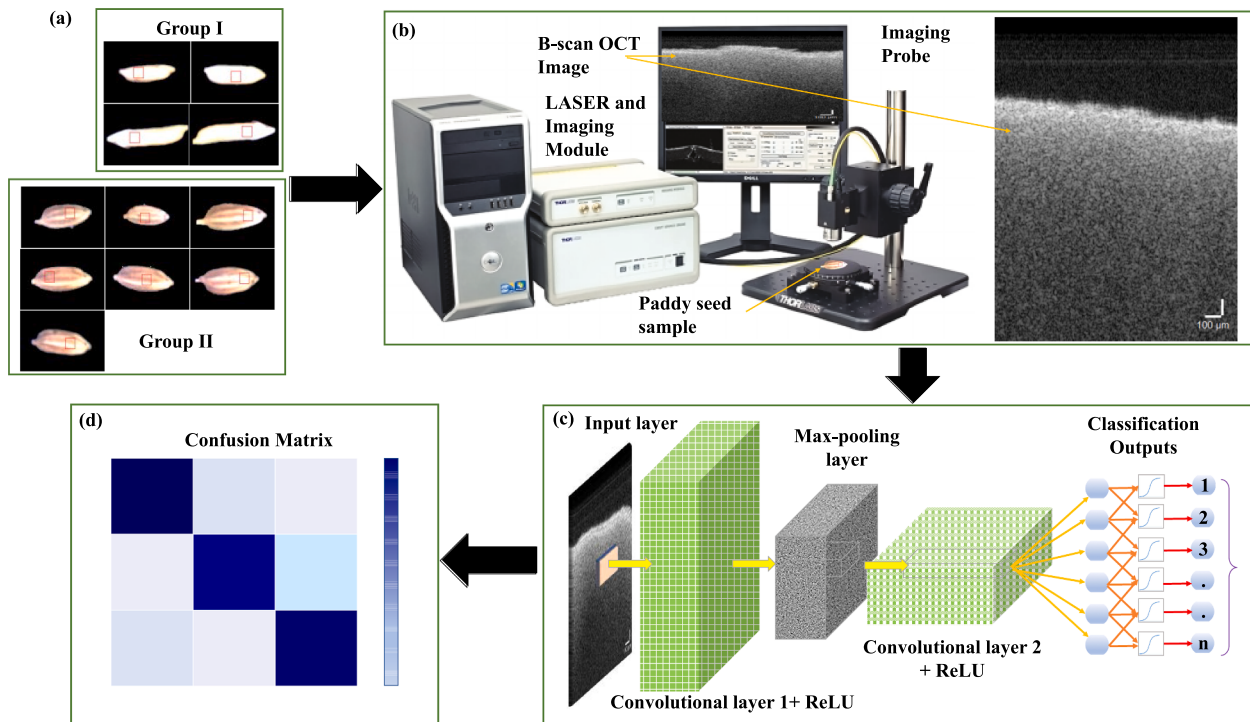


Fig. 3. Workflow diagram showing the steps for classification of OCT images of different seeds (a). Swept-source optical coherence tomography (SS-OCT) set-up is used to acquire B-scan OCT images of the rice seed (b). All B-scan images were taken as an input of (c) Inception-ResNet-V2 architecture is trained 160 seeds (40 for each class) from Group I and 210 seeds (30 for each class) from Group II datasets. The testing results of the network is shown in terms of the confusion matrix (d). Diagonal elements of the matrix represent correct classification while the off-diagonal elements are wrong classification.

into the convolutional layers of the architecture and further classifying it statistically with the help of probability-based fully connected layers [34]. In the present study, we have used a transfer learning approach i.e. using Inception-ResNet-V2 architecture [35], that has been widely used for classifying different datasets [36]. The Inception-ResNet-V2 architecture also known as Inception used 2 different sizes of convolutional filters (3×3 and 5×5) for robust training and extracting all features from the input image. The network consists of total 164 layers i.e. combination of convolution layer, maxpooling, rectifier linear unit (ReLU), softmax and fully connected layer. Mathematical formulation of these layers can be found elsewhere [37]. The physical interpretation of convolution layer is to identify local spatial features across the image. Each filter inside the convolution layer generates one feature map of approximately same size as the input image. Further maxpooling and ReLU is used to clip the output of each convolution layer to make the stable network. The fully connected layer followed by the feature extracting convolutional layers combines the activations of all the neurons in the previous layer. Thus, it computes local, cross-spatial and cross-feature relationships to generate activations for each class. Finally, softmax layer computes the relative activations of all the classes using the softmax function on the activations of the fully connected layer. Lastly, the class label is identified in the output layer as the class for which the softmax function generates the maximum activation.

To train the network, both groups of seed varieties under investigation were categorised as a separate classification problem. Also, each B-scan (2D) image was fed into the architecture as a distinct input. The network was trained separately for Group I and Group II samples. From the acquired volumetric OCT images, all B-scan images from 160 seeds (40 for each class) from Group I and 210 seeds (30 for each class) from Group II datasets is used to train the network. All B-scan images are taken as an individual image to train the network. Total 126,048 B-scan images of Group I (32,000 PUSA Basmati 1, 30,449 PUSA 1509, 31,600 PUSA 44 and 31,999 IR 64) and 40,606 images of Pokkali seeds is used to train the network. In the training procedure, images are taken as an

input of the network where different convolutional layers are used to extract texture and morphological features from the image. After training the network, 32,373 B-scan OCT images of Group I and 15,695 B-scan OCT images of Group II are used for testing purpose. For computational analysis, Matlab 2019a is used on a 64-bit Windows OS, Intel Xeon CPU E5-1650 v4 @ 3.6 GHz with 64 GB RAM and Nvidia 2080 Ti GPU. In each training iteration, the initial learning rate is set as 10-4 and stochastic gradient descent with momentum (SGDM) is used for training. Total 30 epochs are used in the learning process. The training and testing data for both group I & II are given in Table 1.

3. Results and discussion

3.1. OCT imaging and computer vision

In the present investigation, we have used rice seeds primarily because of the presence of vast genetic diversity in rice. The available seed lot is divided into two subsets based on the morphological distinctiveness. The rationale of forming two subsets was to train our machine model on the data emanating from the morphologically distinct seeds and the similar ones. There are many factors that affect seed morphology such as shape, size; and submicron internal structure which can only be visible by using 3D imaging technique. Fig. 4 depicts the B-scan (2D) OCT images acquired from Group I (PUSA Basmati 1, PUSA 1509, PUSA 44 and IR 64) and Group II (BJJ-10-1, BJJ-10-2, BJJ-10-4, BJJ-10-6, BJJ-10-8, BJJ-10-9 and Vyttila 6) datasets. In Fig. 4, X-axis of

Table 1
Training and testing data.

Group I	Seeds	Training	Testing
	160	126,048	32,373
Group II	Seeds	Training	Testing
	210	40,606	15,695

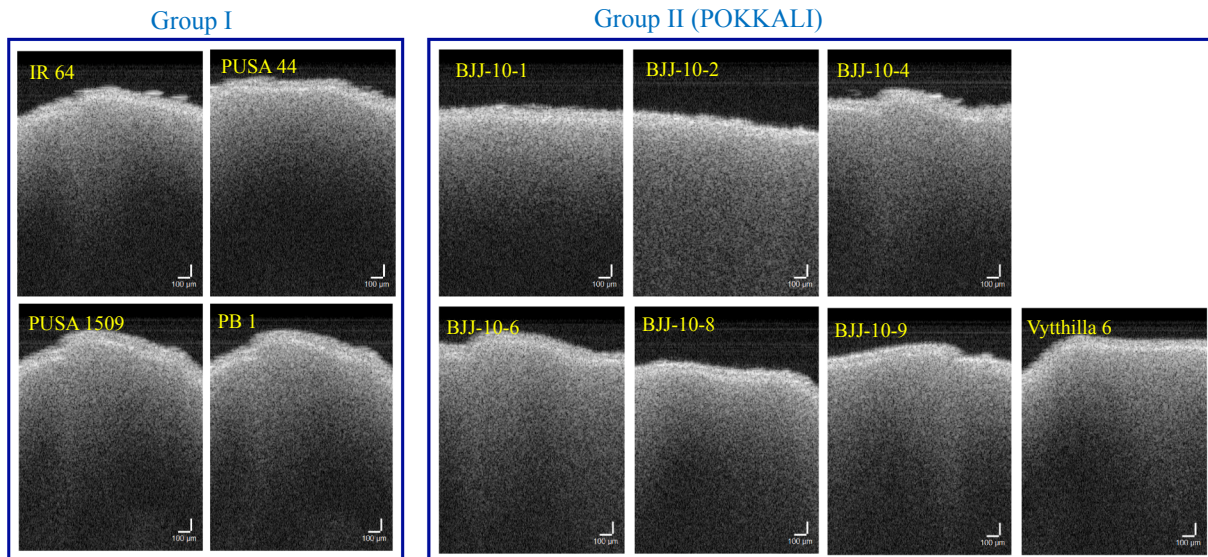


Fig. 4. XZ images of different varieties of Basmati and Pokkali seeds captured by using swept source-optical coherence tomography (SS-OCT).

the image represents the spatial dimension and Y-axis corresponds to the depth of the seed. Our current MEMS-VCSEL SS-OCT system offers high depth of penetration in the biological and agriculture specimens as compare to its counterparts hence best suitable for such type of applications. It can be seen from Fig. 4 that we can achieve approximately 1–1.5 mm depth of penetration in the rice seeds which otherwise is not possible by any conventional non-destructive classification approach.

Group I datasets of Fig. 4 included PUSA Basmati 1, PUSA 1509, PUSA 44 and IR 64 having different shape, length, width and surface area. However, Group II datasets contained morphologically similar Pokkali rice seeds which visibly look similar to each other. Also, it can be seen from the B-scan images of the datasets that they visibly look similar and it is not easy to differentiate them with each other. Nonetheless, it has been shown in the previous study that extracting attenuation coefficient from A-scan (1D) can enable identification of different classes of seeds [38]. Extracting an interpretable feature - attenuation coefficient, from the A-scan for the classification of OCT images is widely used in various biomedical applications [39–41]. A-scan typically shows the depth profile of the sample at particular pixel of the image or at particular position of the sample. The variation in intensity along the depth of the sample is related with the attenuation coefficient of the sample. However, it is very challenging to calculate the value of attenuation coefficient at each point of the sample and then compare it with their counterparts for further analysis. On the other hand, convolutional neural network (CNN) based transfer learning approach does not belong to the interpretable machine learning category. It does not require to extract any physical/interpretable features from the input image [15], but sufficient number of training data is important for the network to learn and differentiate from any other class. The working principle of CNN is that the number of layers inside the network initially generates local spatial and texture features which roughly have the edge information of the input data. After multiple forward and backward propagation of datasets, it highlighted the regions of interests in the images which were used by the network to differentiate it with other images. In other words, the correlation of physical, spatial and texture features extracted from the data is used to divide the samples into their relevant classes.

3.2. Classification result for testing dataset

To perform the classification study, the dataset first splits into training and testing datasets. In this process, total 160 seeds (40 for each class) from Group I and 210 seeds (30 for each class) from Group II

datasets are used to train the network. After sufficient training, 40 seeds (10 from each class) form Group I and 70 seeds (10 for each class) from Group II datasets are used to test the accuracy of the network. The classification accuracy of custom CNN architecture Inception-ResNet-V2 can be seen in terms of confusion matrix (Fig. 5).

The first matrix represents the classification accuracy of rice varieties from Group I. Diagonal elements of the matrix show the correct prediction of the images while the off-diagonal elements are incorrect prediction by the network. For example, it can be inferred from the confusion matrix of four class datasets that total 7,292 images of IR-64 datasets were correctly classified while 800 (85 + 715) images are incorrect predictions, i.e. classified as PUSA 44 and PUSA Basmati 1, respectively. The column on the far right shows the percentage of positive predicted value (PPV), and the bottom row shows true positive rate (TPR) of the network. PPV and TPR can be defined as

$$\text{True positive rate} = \frac{\text{True positive}}{\text{True positive} + \text{False negative}}$$

$$\text{Positive predicted value} = \frac{\text{True positive}}{\text{True positive} + \text{False positive}}$$

From the confusion matrix of four class rice datasets that per class classification accuracy of IR 64, PUSA 44, PUSA 1509 and PUSA Basmati 1 is found to be 90.1%, 92.9%, 88.2% and 87.2% respectively. The overall accuracy in the bottom right of the matrix represents the average value of per class accuracy. Classification accuracy of Group II seeds is also depicted in Fig. 5. The overall classification accuracy in identifying the four rice seed varieties in Group I and seven morphologically similar varieties of Pokkali seeds mentioned in Group II is achieved to be 89.6% and 82.5%, respectively. The accuracy of the network decreased by increasing the number of classes in the datasets. Also, it might be possible that classification accuracy decreased due to similar morphology of group II datasets, especially for BJJ 10-8 type of rice seeds. The classification accuracy of BJJ 10-8 is found very less i.e. only 14.6%. The variety mostly matched with BJJ-10-9 and Vythilla 6 type of rice seeds. In contrast, BJJ 10-1 is the most accurate identified variety by the proposed framework with an accuracy of 100%. Nonetheless, the overall accuracy of 89.6% 82.5% of large OCT datasets for different rice seeds shows the potential of current framework for the current framework for the classification of even morphologically similar seed variety.

Further, DNA profiling based on randomly chosen seven hyper variable simple sequence repeat markers (HvSSRs) is performed in Group I type of seeds (Fig. 6). Although HvSSRs used in the present study were

		Target Class						Positive predicted value
		Rice Seed	IR 64	PUSA 44	PUSA 1509	PUSA Basmati 1		
Output Class	IR 64	7293 22.5%	67 0.0%	1 0.0%	147 0.0%	97.1% 2.9%		
	PUSA 44	85 0.0%	7522 23.2%	650 0.0%	16 0.0%	90.9% 9.1%		
	PUSA 1509	0 0.0%	498 0.0%	7135 21.8%	867 0.1%	83.9% 16.1%		
	PUSA Basmati 1	715 0.1%	6 0.0%	307 0.0%	7043 21.8%	87.3% 12.7%		
	True Positive Rate	90.1% 9.9%	92.9% 7.1%	88.2% 11.8%	87.2% 12.8%	89.6% 10.4%		

Fig. 5. Confusion matrices represent the true positive rate, positive predicted value and overall classification accuracies of the Inception-ResNet-V2 network for the classification of different seeds.

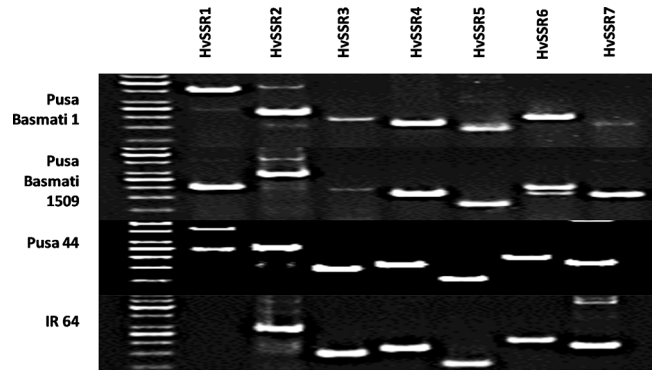


Fig. 6. DNA profiling of four selected rice varieties (Group I) using seven hyper variable SSR markers (HvSSRs).

able to clearly establish the identity of Pusa Basmati 1 and Pusa Basmati 1509 but the DNA profile of IR64 and PUSA 44 were indistinguishable suggesting screening for more HvSSR markers for generating discernible fingerprints. We expect that the use of more HvSSR might result into a unique profile for all the varieties, but it will also add on the total cost of varietal identification. Similarly, it might help to identify Group II seed variety, but the cost and seed variety identification time will be much higher than our proposed technique. In this context, we propose that our method of varietal identification presented here is far more robust and facile than other methods.

After training of the architecture with desired varieties, the trained model can directly be used for the identification of the seed variety with individual OCT image. It takes only 2–3 s to capture a 2D OCT image of a single seed and another few milliseconds for the trained Inception-ResNet-V2 model for identification on a general computer system. By capturing the OCT images of the same seed at multiple locations, the probability of correct identification can be increased. Hence, the proposed approach is a rapid, robust and easy-to-use methodology for seed identification. It can be implemented in the gene banks to tackle the duplication issue in morphologically similar seed varieties. The proposed OCT + deep learning framework can further be used for the identification of admixed variety with appropriate training. It can potentially be applied in the seed retail shops and consumer stores for quality control purposes.

Pokkali Seed	Target Class							Positive predicted value
	BJJ 10-1	BJJ 10-2	BJJ 10-4	BJJ 10-6	BJJ 10-8	BJJ 10-9	Vytthilla 6	
BJJ 10-1	2122 13.5%	0 0.0%	0 0.0%	24 0.2%	22 0.1%	0 0.0%	0 0.0%	97.9% 2.1%
BJJ 10-2	0 0.0%	1978 12.6%	3 0.0%	0 0.0%	3 0.0%	0 0.0%	0 0.0%	99.7% 0.3%
BJJ 10-4	0 0.0%	143 0.9%	2118 13.5%	0 0.0%	98 0.6%	0 0.0%	0 0.0%	89.8% 10.2%
BJJ 10-6	0 0.0%	0 0.0%	0 0.0%	3007 19.2%	0 0.0%	0 0.0%	0 0.0%	100% 0.0%
BJJ 10-8	0 0.0%	0 0.0%	0 0.0%	0 0.0%	306 1.9%	0 0.0%	0 0.0%	100% 0.0%
BJJ 10-9	0 0.0%	0 0.0%	0 0.0%	0 0.0%	526 3.4%	1368 8.7%	52 0.3%	70.3% 29.7%
Vytthilla 6	0 0.0%	0 0.0%	0 0.0%	0 0.0%	1145 7.3%	732 4.7%	2048 13.0%	52.2% 47.8%
True Positive Rate	100% 0.0%	93.3% 6.7%	99.9% 0.1%	99.2% 0.8%	14.6% 85.4%	65.1% 34.9%	97.5% 2.5%	82.5% 17.5%

4. Conclusions

The main objective of this study was to develop a system which can complement the process of DNA fingerprinting. It can be used where the DNA profile of different varieties is not very distinct as this is the case when a variety is a very similar selection of its parent. For instance, pokkali varieties are very similar not only morphologically but also at DNA level. In such cases development of a unique fingerprint is a real challenge. In this study, we demonstrated a rapid, robust and non-destructive imaging approach, SS-OCT with CNN for accurate classification of morphologically similar varieties of paddy seeds. Total four varieties of long-grain rice seeds (PUSA 44, PUSA 1509, IR 64 and PUSA Basmati 1) and seven morphologically similar varieties of rice landrace Pokkali seeds (BJJ-10-1, BJJ-10-2, BJJ-10-4, BJJ-10-6, BJJ-10-8, BJJ-10-9 and Vyttila 6) were imaged in the present investigation. SS-OCT system offers unique advantages over other proposed systems for seed imaging that includes fast acquisition and sub-surface imaging of the sample. Further, a deep learning architecture, Inception-ResNet-V2 was used to classify the OCT images of the seeds into their relevant classes. After sufficient training of the network, it demonstrates an excellent accuracy against the test datasets. Targeting four to seven class of problems, it provides an average accuracy of 89.6% and 82.5% while differentiating between morphologically different and morphologically similar rice seeds, respectively.

Further, we propose that our current approach can be used in conjunction of DNA fingerprinting to reduce to overall cost of varietal identification. For instance, while developing DNA profile of the Group I varieties using seven HvSSR markers we found that the DNA profile of IR64 and PUSA 44 were indistinguishable suggesting screening for more HvSSR markers for generating discernible fingerprints leading to increase in the overall cost of varietal identification. However, by processing the OCT images with Deep learning architecture are able to easily classify the IR64 and PUSA 44 seeds varieties. Moreover, the accuracy of our classification framework is expected to increase with the volume of data and thus more than 95% classification accuracy is anticipated by gradual refinements. The significant high accuracy obtained with this rapid and robust methodology suggests that it has a potential of being developed as a reliable tool for varietal identification of rice and other cereal grains. Finally, we conclude that the proposed method has a much wider application in applied research, seed industry, gene banks, and plant quarantine laboratories.

CRediT authorship contribution statement

Deepa Joshi: Project administration, Conceptualization, Methodology, Investigation, Writing - review & editing, Funding acquisition. **Ankit Butola:** Data curation, Methodology, Writing - review & editing. **Sheetal Raosaheb Kanade:** Investigation, Writing - review & editing, Formal analysis, Data curation. **Dilip K. Prasad:** Data curation. **S.V. Amitha Mithra:** Project administration. **N.K. Singh:** Project administration. **Deepak Singh Bisht:** Investigation, Writing - review & editing. **Dalip Singh Mehta:** Project administration, Supervision, Validation, Funding acquisition.

Declaration of Competing Interest

The authors declare that they have no known competing financial interests or personal relationships that could have appeared to influence the work reported in this paper.

Acknowledgement

Author DJ is thankful to Department of Science & Technology (DST), Government of India for the Women Scientist (WOSA) fellowship grant SR/WOS-A/PM-19/2018.

References

- [1] F.C. Correa, F.S.D. Silva, C. Jaren, P.C.A. Junior, I. Arana, Physical and mechanical properties in rice processing, *J. Food Eng.* 79 (2006) 137–142.
- [2] D. Tilman, C. Balzer, J Hill BL Befort, Global food demand and the sustainable intensification of agriculture, *Proc. Natl. Acad. Sci. USA* 108 (2011) 20260–20264.
- [3] K.P. Voss-Fels, A. Stahl, L.T. Hickey, Q&A: Modern crop breeding for future food security, *BMC Biol. BioMed Central Ltd.* 18 (2019).
- [4] N. Singh, S. Wu, W.J. Raupp, S. Sehgal, S. Arora, V. Tiwari, et al., Efficient curation of genebanks using next generation sequencing reveals substantial duplication of germplasm accessions, *Sci Rep.* 9 (2019) 650.
- [5] K. Weising, H. Nybom, K. Wolff, G. Kahl, *DNA Fingerprinting in Plants: Principles Methods, and Applications*, CRC Press, 2005.
- [6] H. Nybom, K. Weising, B. Rotter, DNA fingerprinting in botany: past, present, future, *Investig. Genet.* 5 (2014) 2223–2225.
- [7] P. Punthumast, Y. Auttawaitkul, W. Chiracharit and K. Chamnongthai, Non-destructive identification of unmilled rice using digital image analysis, in: 9th International Conference on Electrical Engineering/Electronics Computer Telecommunications and Information Technology (ECTI-CON),, 2012, pp. 1–4.
- [8] P. Barreiro, et al., Non-destructive seed detection in mandarins: Comparison of automatic threshold methods in FLASH and COMSPIRA MRIs, *Postharvest Biol. Technol.* 47 (2008) 189–198.
- [9] S. Jahnke, et al., Combined MRI–PET dissects dynamic changes in plant structures and functions, *Plant J.* 59 (2009) 634–644.
- [10] S. Sankaran, A. Mishra, R. Ehsani, C. Davis, A review of advanced techniques for detecting plant diseases, *Comput. Electron. Agric.* 72 (2010) 1–13.
- [11] M. Shahin, E. Tollarer, R. McClendon, H. Arabia, Apple classification based on surface bruises using image processing and neural networks, *Trans. ASAE* 45 (2002) 1619.
- [12] J. Chen, M. Li, T. Pan, L. Pang, L. Yao, J. Zhang, Rapid and non-destructive analysis for the identification of multigrain rice seeds with near-infrared spectroscopy, *Spectrochim. Acta A Mol. Biomol. Spectrosc.* 219 (2019) 179–185.
- [13] L. Feng, S. Zhu, F. Liu, Y. He, Y. Bao, C. Zhang, Hyperspectral imaging for seed quality and safety inspection: a review, *Plant Methods BioMed. Central* 15 (2019) 1–25.
- [14] Z. Qiu, J. Chen, Y. Zhao, S. Zhu, Y. He, C. Zhang, Variety Identification of Single Rice Seed Using Hyperspectral Imaging Combined with Convolutional Neural Network, *Appl. Sci.* 8 (2018) 212–224.
- [15] A. Butola, A. Ahmad, V. Dubey, V. Srivastava, D. Qaiser, A. Srivastava, et al., Volumetric analysis of breast cancer tissues using machine learning and swept-source optical coherence tomography, *Appl. Opt.* 58 (A) (2019) 135–141.
- [16] S.P.K. Karri, D. Chakraborty, J. Chatterjee, Transfer learning based classification of optical coherence tomography images with diabetic macular edema and dry age-related macular degeneration, *Biomed. Opt. Express* 8 (2017) 579–592.
- [17] J. De Fauw, J.R. Ledsam, B. Romera-Paredes, S. Nikolov, N. Tomasev, S. Blackwell, et al., Clinically applicable deep learning for diagnosis and referral in retinal disease, *Nat. Med.* 24 (2018) 1342–1350.
- [18] W. Drexler, J.G. Fujimoto, *Optical coherence tomography: Technology and applications*, second ed., Springer International Publishing, 2015.
- [19] T. Anna, S. Chakraborty, C.Y. Cheng, V. Srivastava, A. Chiou, W.C. Kuo, Elucidation of microstructural changes in leaves during senescence using spectral domain optical coherence tomography, *Sci. Rep.* 9 (2019) 1–10.
- [20] V. Srivastava, D. Dalal, A. Kumar, S. Prakash, K. Dalal, In vivo automated quantification of quality of apples during storage using optical coherence tomography images, *Laser Phys.* 28 (2018) 1–8.
- [21] S.Y. Lee, C. Lee, J. Kim, H.Y. Jung, Application of optical coherence tomography to detect Cucumber green mottle mosaic virus (CGMMV) infected cucumber seed, *Hortic Environ. Biotechnol.* 53 (2012) 428–433.
- [22] I.V. Meglinski, C. Buranachai, L.A. Terry, Plant photonics: Application of optical coherence tomography to monitor defects and rots in onion, *Laser Phys. Lett.* 7 (2010) 307–310.
- [23] J.K. Manattayil, N.K. Ravichandran, R.E. Wijesinghe, M.F. Shirazi, S.-Y. Lee, P. Kim, et al., Non-destructive classification of diversely stained capsicum annuum seed specimens of different cultivars using near-infrared imaging based optical intensity detection, *Sensors* 18 (2018) 2500.
- [24] R.E. Wijesinghe, Seung-Yeol Lee, Naresh Kumar Ravichandran, Muhammad Faizan Shirazi, Pilun Kim, Hee-Young Jung, Mansik Jeon, Jeehyun Kim, Biophotonic approach for the characterization of initial bitter-rot progression on apple specimens using optical coherence tomography assessments, *Sci. Rep.* 8 (2018) 15816.
- [25] V.V. Sapozhnikova, I.S. Kutis, S.D. Kutis, R.V. Kuranov, G.V. Gelikonov, D.V. Shabanov, V.A. Kamensky, In vivo monitoring of seeds and plant-tissue water absorption using optical coherence tomography and optical coherence microscopy, in: *Proceedings Coherence Domain Optical Methods and Optical Coherence Tomography in Biomedicine VIII*, vol. 5316, 2004. Event: Biomedical Optics, San Jose, CA, United States, 2004, <https://doi.org/10.1117/12.528515>.
- [26] H. Kim, X. Du, S. Kim, P. Kim, R.E. Wijesinghe, B.J. Yun, K.M. Kim, M. Jeon, M. J. Kim, Non-invasive morphological characterization of rice leaf bulliform and Aerenchyma cellular regions using low coherence interferometry, *Appl. Sci.* 9 (2019) 2104.
- [27] Bharti, T. Yoon, B. Lee, Identification of fungus-infected tomato seeds based on full-field optical coherence tomography, *Curr. Opt. Photon.* 3 (2019) 571–576.
- [28] <https://www.thorlabs.com/thorproduct.cfm?partnumber=OCS1310V1>.
- [29] A. Butola, D.K. Prasad, A. Ahmad, V. Dubey, D. Qaiser, A. Srivastava, et al., Deep learning architecture LightOCT for diagnostic decision support using optical coherence tomography images of biological samples, 11 (2020) 5017–5031.
- [30] <https://se.mathworks.com/help/deeplearning/ref/plotconfusion.html>.
- [31] A.A. Chaugule, S.N. Mali, Identification of paddy varieties based on novel seed angle features, *Comput. Electron. Agric.* 123 (2016) 415–422.
- [32] X. Chen, Y. Xun, W. Li, J. Zhang, Combining discriminant analysis and neural networks for corn variety identification, *Comput. Electron. Agric.* 71 (2010) S48–S53.
- [33] B. Lurstwut, C. Pornpanomchai, Image analysis based on color, shape and texture for rice seed (*Oryza sativa L.*) germination evaluation, *Agric. Nat. Resour.* 51 (2017) 383–389.
- [34] Y. Lecun, Y. Bengio, G. Hinton, Deep learning, *Nature* 521 (2015) 436–444.
- [35] A. Butola, D. Popova, D.K. Prasad, A. Ahmad, J. Habib, J. Claude Tinguely, P. Basnet, G. Acharya, P. Senthilkumar, D.S. Mehta, B.S. Ahluwalia, High spatially sensitive quantitative phase imaging assisted with deep neural network for classification of human spermatozoa under stressed condition 10 (2020) 13118.
- [36] C. Szegedy, S. Ioffe, V. Vanhoucke, A.A. Alemi, Inception-v4, Inception-ResNet and the impact of residual connections on learning, in: *Proceedings of the Thirty-First AAAI Conference on Artificial Intelligence (AAAI-17)*, 4278–7284.
- [37] I. Goodfellow, Y. Bengio, A. Courville, *Deep Learning*, MIT Press, 2016.
- [38] T. Jiang, Y. Zhang, F. Cai, J. Qian, S. He, Optical coherence tomography for identifying the variety of rice grains, in: *2010 OSA-IEEE-COS Adv Optoelectron Micro/Nano-Optics, AOM 2010*, pp. 0–2.
- [39] S. Liu, Tissue characterization with depth-resolved attenuation coefficient and backscatter term in intravascular optical coherence tomography images, *J. Biomed. Opt.* 22 (2017) 1–16.
- [40] R.A. McLaughlin, L. Scolaro, P. Robbins, C. Saunders, S.L. Jacques, D.D. Sampson, Mapping tissue optical attenuation to identify cancer using optical coherence tomography, *Med. Image Comput. Assist. Interv.* 12 (2009) 657–664.
- [41] F. van der Meer, D.J. Faber, D.M. Baraznjii Sasoon, M.C. Aalders, G. Pasterkamp, T. G. van Leeuwen, Localized measurement of optical attenuation coefficients of atherosclerotic plaque constituents by quantitative optical coherence tomography, *IEEE Trans. Med. Imaging.* 24 (2005) 1369–1376.